Available online at www.sciencedirect.com
ScienceDirect
Biochemical and Biophysical Research Communications 356 (2007) 187–192
BBRC
www.elsevier.com/locate/ybbrc

Fast cortical oscillation after thalamic degeneration: Pivotal role of NMDA receptor

Shin-ichi Kyuhou *, Hisae Gemba

Department of Physiology, Kansai Medical University, Moriguchi, Osaka 570-8506, Japan

Received 26 January 2007
Available online 1 March 2007

Abstract

We examined electrophysiological and molecular changes of the thalamocortical system after thalamic degeneration in Purkinje cell degeneration (pcd) mice. In pcd mice, neurons in specific thalamic nuclei including the ventral medial geniculate nucleus began to degenerate around postnatal day 50, whereas the visual thalamic nucleus and nonspecific thalamic nuclei remained almost intact. In association with the morphological changes, auditory evoked potentials in the primary auditory cortex (AC) began to decrease gradually. Fast Fourier transform analysis of spontaneous cortical field potentials revealed that fast oscillation (FO) around 25 Hz occurred in the AC but not in the visual cortex. Quantitative mRNA analysis demonstrated that expression of the *N*-methyl-D-aspartate (NMDA) receptor was up-regulated in the AC but not in the visual cortex. Systemic administration of an NMDA antagonist abolished the FO in the AC. These results indicate that increased NMDA activity may cause the FO in the AC of pcd mice.

Keywords: Neurodegeneration; Auditory thalamus; NMDA receptor; Fast oscillation; Auditory evoked potentials; Synapse; Fast Fourier transform

Purkinje cell degeneration (pcd) mice were first identified as mutant mice having cerebellar ataxia due to degeneration of cerebellar Purkinje cells [1]. This degeneration of Purkinje cells was found to involve endoplasmic reticulum stress and activation of microglia [2]. Additional studies have shown that not only the cerebellar neurons but also thalamic neurons degenerate in pcd mice [3,4]. The thalamus is a large relay station of sensory, motor, and association information. It also acts a rhythm generator for cortical oscillation [5]. Previous studies [3,4] have thoroughly investigated the morphological changes during degeneration of the thalamocortical system, but the electrophysiological and molecular changes have not been investigated. The thalamic degeneration in pcd mice is not diffuse but particular thalamic nuclei selectively degenerate. The ventral medial geniculate nucleus, the main auditory thalamic nucleus, is one of the degenerating thalamic nuclei. Thus, we predicted the decrement of the auditory responses. While confirming the prediction, we found that fast oscillation (FO) appeared in the auditory cortex (AC) and *N*-methyl-D-aspartate (NMDA) receptors were involved in this oscillation. The NMDA receptors play important roles in activity-dependent changes in synaptic strength and connectivity that are thought to underlie neuronal development and reorganization [6–8]. These biologically important receptors are tetramers composed of the ubiquitous NR1 subunit and various combinations of NR2 or NR3 subunits. The subunit composition of each receptor complex controls its functional properties. In the current study, we investigated the changes in the expression of the NMDA receptors in the thalamocortical system by quantitative real-time polymerase chain reaction (PCR), and we confirmed their role in generation of FO using a pharmacological agent.

Materials and methods

Animals. Pcd mice of either sex ($n = 23$; postnatal days [*P*] 38–80) and wild-type (wt) C57/B6j mice ($n = 10$) (Jackson Lab, Bar Harbor, ME)

* Corresponding author. Fax: +81 6 69921770.
E-mail address: kyuho@takii.kmu.ac.jp (S. Kyuhou).

0006-291X/$ - see front matter © 2007 Elsevier Inc. All rights reserved.
doi:10.1016/j.bbrc.2007.02.116

were used in the present study. All procedures were approved by the Animal Experimentation Committee of Kansai Medical University.

Morphological studies. Mice were transcardially perfused with 4% paraformaldehyde in 0.1 M Na-phosphate-buffered saline (PBS). The brains were removed and postfixed overnight at 4 °C using the same fixative and then cut into 20-μm coronal sections using a freezing microtome. For most brains, every fifth section was stained with neutral red, and the next three sections were used for immunochemical analysis or were stained with Fluoro-Jade B [9]. The thalamic nuclei were identified according to their cytoarchitecture [10] and by immunostaining of calbindin and parvalbumin as described previously [11,12].

For immunochemical studies, sections were incubated for 30 min with PBS containing 1% bovine serum albumin and then reacted overnight at 4 °C with mouse anti-calbindin or anti-parvalbumin monoclonal antibodies (Sigma, St. Louis, MO). Sections were rinsed with PBS and incubated with biotin-conjugated anti-mouse antibody (Jackson ImmunoResearch Laboratories, West Grove, PA). For bright-field microscopy, sections were treated with the appropriate biotin-conjugated secondary antibody, incubated with avidin–biotin complex (Vectastain Elite ABC-Peroxidase kit; Vector Laboratories, Burlingame, CA), and reacted with diaminobenzidine. DNA fragmentation was visualized by terminal transferase and fluorescein-dUTP (Dead-end colorimetric TUNEL system; Promega, Madison, WI) according to the manufacturer's instructions.

To specifically stain degenerating neurons, sections were stained with Fluoro-Jade B as described by Schmued [9]. Briefly, the sections were first immersed in a solution containing 1% sodium hydroxide in 80% alcohol and then incubated for 2 min in 70% alcohol followed by 2 min in distilled water. The sections were then transferred to a solution of 0.06% potassium permanganate for 10 min and then rinsed in distilled water for 2 min. The staining solution was prepared from a 0.001% stock solution of Fluoro-Jade B in 0.1% acetic acid. Sections were incubated in Fluoro-Jade B for 20 min, air-dried, and coverslipped. Stained sections were observed with a confocal laser microscope (Fluoview, Olympus, Tokyo, Japan).

Electrophysiological studies. Stainless steel electrodes (0.05 mm in diameter), insulated except at their tips, were placed on the surface and at a depth of 1.0 mm in the primary auditory cortex (AC) and at depth of 0.6 mm in the visual cortex (VC) under urethane anesthesia (1.0 g/kg by intraperitoneal injection). Two silver wires were implanted in the bone behind the ears on both sides and used as indifferent electrodes. For systemic injection of MK801, the drug was administered intraperitoneally (0.3 mg/kg). All electrodes were affixed to two screws (1-mm diameter) in the skull with dental cement.

One week after the surgery, mice were placed in a chronic head holder to painlessly restrain their heads, and recordings were started. The mice rapidly adjusted to the restraint. The mice received sequential auditory stimuli from a speaker every 2 s. The auditory stimulus was usually a 1-ms click at 80 dB sound pressure level with a decay time of 0.2 ms. Cortical field potentials were recorded and amplified with bandpass filter of 0.05–100 Hz. Amplified signals from 100 click stimuli were fed into a computer at sampling rate of 1 kHz and were averaged at the onset of the stimulus. For auditory brainstem response measurements, 0.1-ms click stimuli were used. Auditory brainstem response waveforms were recorded for 10 ms at a sampling rate of 5 kHz using a 100–3000 Hz bandpass filter. Waveforms from 1000 stimuli were averaged. Auditory brainstem response waveforms were recorded in decreasing 10-dB intervals starting from a maximum amplitude of 90 dB until no waveform could be observed. After recordings, the animals were sacrificed by intraperitoneal injection with an overdose of pentobarbital (100 mg/kg), and the locations of the electrodes were examined histologically.

Quantitative real-time PCR. Total RNA was extracted from the thalamus and cerebral cortex as described previously [2]. The isolated RNA samples were treated with RNase-free DNase I (Qiagen, Valencia, CA) for 30 min at 37 °C to remove any contaminating genomic DNA. First-strand cDNA was generated from the RNA samples using reverse transcriptase (Applied Biosystems, Foster City, CA) and random hexamer primers. The cDNA samples were amplified in a real-time fluorescence thermal cycler (Opticon2; MJ Research, Waltham, MA) using the appropriate primers (10 μM) and *Taq* DNA polymerase mixture (Takara, Ohtu, Japan) containing the DNA-sensitive fluorescent dye SYBR Green I® (Molecular Probes, Eugene, OR). Amplification reactions were conducted for 50 cycles of denaturation for 15 s at 94 °C, annealing for 3 s at 60 °C, and extension for 15 s at 72 °C. Fluorescence was measured during the extension phase of each cycle. The following primer sequences were used: for NR1, 5′-TGAGTCCAAGGCAGAGAAGG-3′ (sense) and 5′-TCG CTTGCAGAAAGGATGAT-3′ (antisense); for NR2A [13], 5′-GGA AGTTGGACGCTTTCATC-3′ (sense) and 5′-TCTTCCATCTCACCGT CACC-3′ (antisense); for NR2B, 5′-TGCTACAACACCCACGAGAA-3′ (sense) and 5′-TCTCCCACTTCCTCTCCTTG-3′ (antisense); for NR2C, 5′-TCTCACCAAGGGCAAGAAGT-3′ (sense) and 5′-CGAGGAAGA TGACAGCGAAG-3′ (antisense); for NR2D, 5′-CTGTGGGCTATA ACCGAAGC-3′ (sense) and 5′-CCATGATCTTGCTGGTGGT-3′ (antisense); and for glyceraldehyde 3-phosphate dehydrogenase (GAPDH), 5′-CATACACCACCACACCTGAAAG-3′ (sense) and 5′-CCGTTTCC TAGTTCTTCCTTGC-3′ (antisense) [14]. The predicted sizes of the PCR products for NR1, NR2A, NR2B, NR2C, NR2D, and GAPDH were 114, 202, 163, 167, 150, and 380 bp, respectively. After real-time PCR procedures, the lengths of the PCR products were confirmed by electrophoresis on an ethidium bromide-stained 2% agarose gel and photography under UV illumination. Part of results of real-time PCR using SYBR Green I were confirmed using Taqman® gene expression assays (Mm99999915_g1 for GAPDH and Mm00433820_m1 for NR2B; Applied Biosystems), which measure the amount of cDNA using the other fluorescent probes.

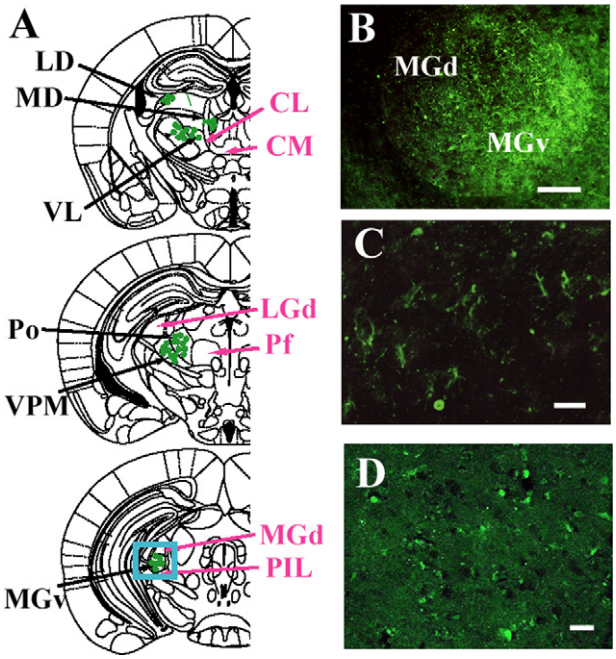

Fig. 1. Detection of degenerating neurons in the thalamus of pcd mice. (A) Location of Fluoro-Jade-positive thalamic neurons plotted on line drawings of the coronal sections as adopted from the mouse brain atlas [10]. Each green dot indicates approximately 10 labeled cells. The labeled thalamic neurons are distributed as follows: LD, laterodorsal nucleus; MD, mediodorsal nucleus; VL, ventrolateral nucleus; Po, posterior complex; VPM, posterior ventromedial nucleus; MGv, ventral medial geniculate nucleus. The thalamic nuclei, which contain few degenerating cells, are shown on the right side (red) as follows: CL, central lateral nucleus; CM, central medial nucleus; LGd, dorsal lateral geniculate nucleus; Pf, parafascicular nucleus; MGd, dorsal medial geniculate; PIL, posterior intralaminar nucleus. (B) Fluorescent photomicrograph showing degenerating neurons stained by Fluoro-Jade (green) in the MGv, which was indicated with a blue rectangle in (A). (C) Higher magnification of the image in (B). (D) DNA fragmentation was detected by the TUNEL method (green) in the MGv at P60. Scale bar = 200 μm in (B) and 50 μm in (C) and (D).

Results

We initially used Fluoro-Jade B staining to localize degenerating neurons in pcd mice. At P40, degenerating thalamic neurons were not observed. At P47, a few degenerating thalamic neurons could be detected in the mediodorsal and MGv nuclei. After P50, many degenerating thalamic neurons were present in the laterodorsal, mediodorsal, submedial, ventrolateral, and posterior ventromedial nuclei as well as the posterior complex and the MGv (Fig. 1A–C), which are specific thalamic nuclei. These neurons contained atrophic somas and condensed chromatin and were stained by TUNEL (Fig. 1D), suggesting that they were undergoing apoptosis. In contrast, degenerating neurons were rarely observed in the central lateral, central medial, ventromedial, parafascicular, dorsal, posterior intralaminar, or dorsal medial geniculate nuclei, which are nonspecific thalamic nuclei (Fig. 1A). Degenerating neurons also were not found in the dorsal lateral geniculate nuclei (LGd), which project to the VC.

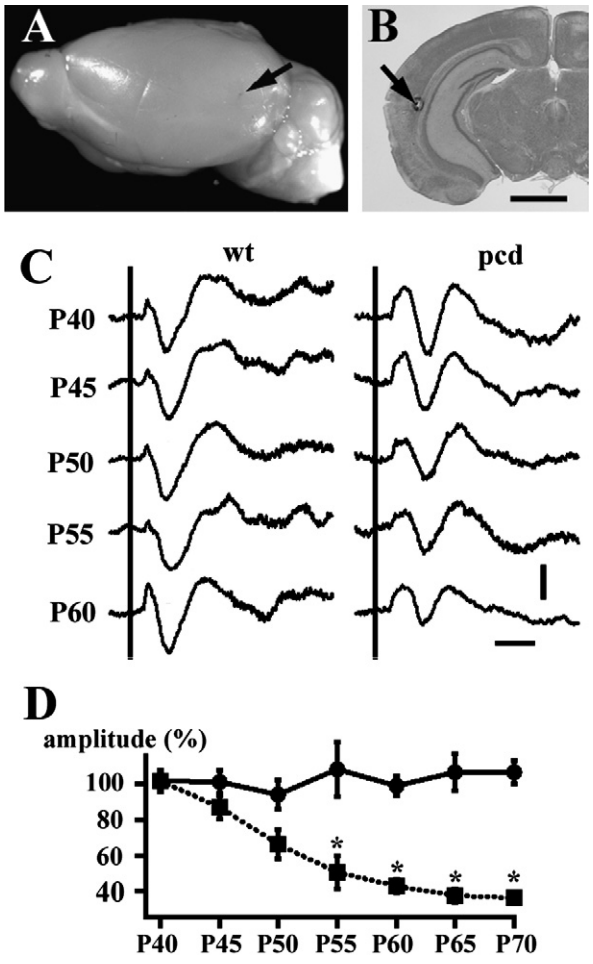

Fig. 2. Decrement of auditory responses in pcd mice. (A) Location of the electrode in the AC (arrow). (B) Coronal section of the brain. The tip of the deep electrode was labeled by iron deposition (arrow). (C) Postnatal changes of transcortical AEPs in the AC of wt (left columns) and pcd (right columns) mice. Numerals on the left side indicate the postnatal day. (D) Time course of the amplitude of the transcortical AEPs in wt ($n = 3$) and pcd ($n = 3$) mice at a latency of 20 ms. The amplitude of the AEPs was normalized by that at P40. Plotted values indicate means ± SEM. Asterisks indicate statistically significant differences as determined by a t-test ($P < 0.05$). Scale bar = 1 mm in (B), 0.1 mV and 20 ms in (C).

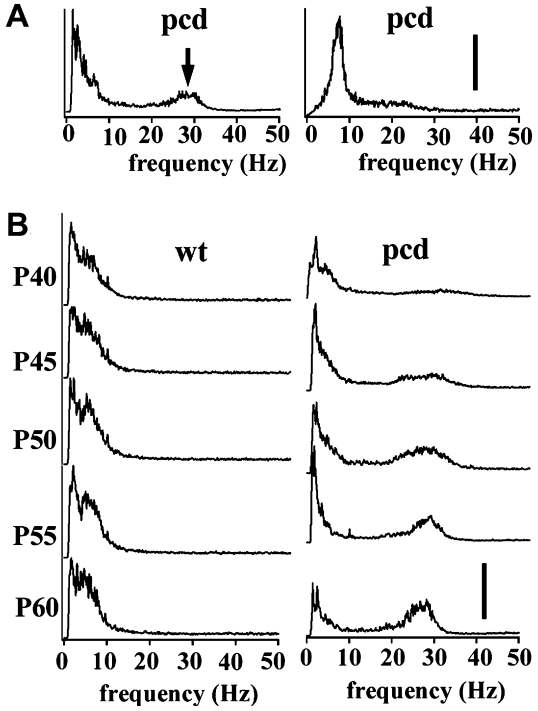

Fig. 3. Appearance of oscillatory activities associated with thalamic degeneration. (A) Fast Fourier transform analysis of the transcortical field potentials in the AC (left trace) and VC (right trace) of pcd mice at P50. Note that FO appeared in the AC (arrow) but not in the VC. (B) Fast Fourier transform analysis of the spontaneous transcortical field potentials in the AC of wt (left columns) and pcd (right columns) mice. Numerals on the left side indicate the postnatal day. Scale bar = 0.1 mV in (A) and 0.1 mV^2/Hz in (B).

Decrease in auditory evoked potentials (AEPs) in pcd mice

We next measured AEPs using electrodes chronically implanted on the surface and at a depth of 1.0 mm in the AC (Fig. 2A and B). We observed prominent AEPs from both electrodes in the wt and pcd mice. Transcortical (surface potential minus depth potential) recordings can eliminate the volume conducting potentials and correctly measure the local electrical activities (Fig. 2C). From P40 to P70, the waveforms and amplitudes of the AEPs remained unchanged in the wt mice, whereas starting at P50 in the pcd mice, the component of AEPs at a peak latency of 20 ms began to decrease gradually (Fig. 2C and D). Because a few degenerating neurons were distributed in the inferior colliculus, it is possible that the decrease in the AEP was caused by the dysfunction at the brainstem level; however, the amplitude and waveforms of the auditory brainstem response remain unchanged, indicating that the decrease in the AEPs was mostly due to the degeneration of the thalamic neurons.

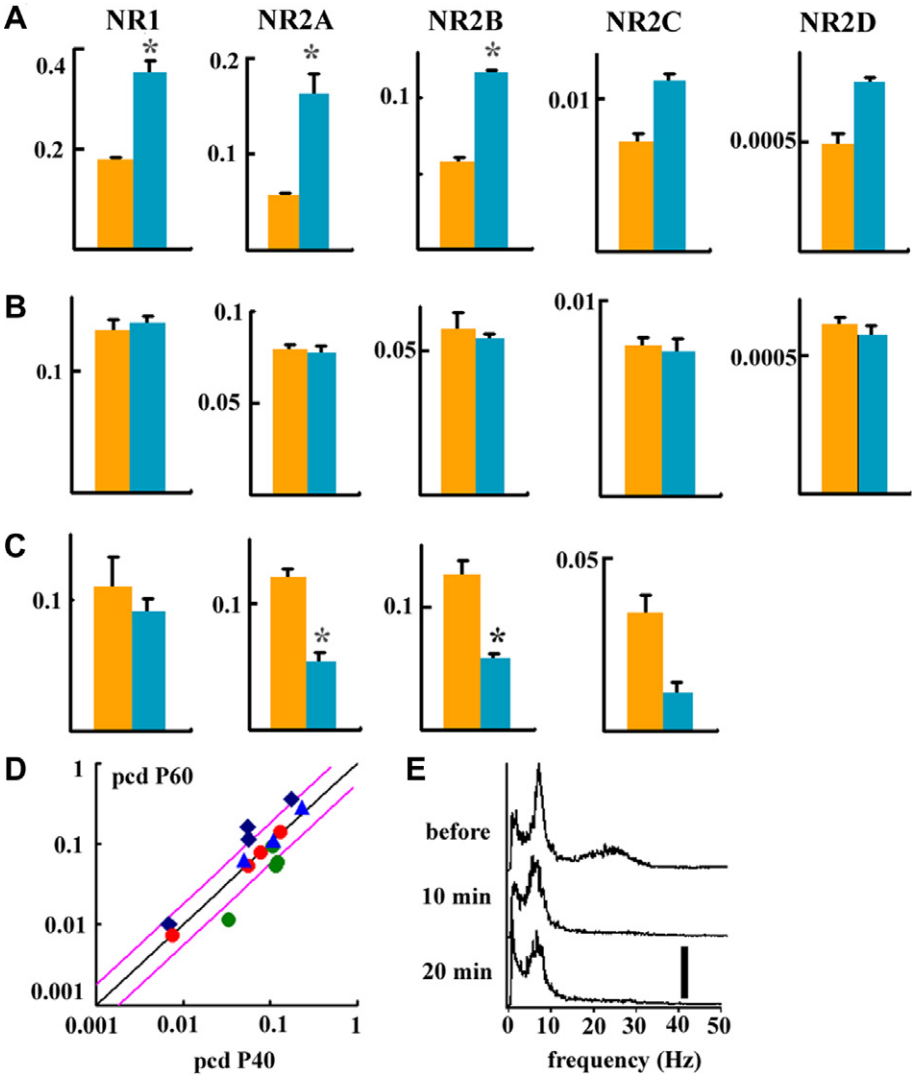

Fig. 4. Involvement of NMDA receptors in the occurrence of FO. (A) Expression of NMDA receptors in the pre-degenerating period (P40) and degenerating period (P60) of pcd mice. Levels of NR1, NR2A, NR2B, NR2C, and NR2D transcripts in the AC of P40 (orange columns) and P60 (blue columns) mice. The ordinate indicates the transcript levels normalized by the GAPDH transcript level ($n = 4$ per group). Plotted values indicate means ± SEM. $^{*}P < 0.05$. (B) Expression of NMDA receptors in the VC. (C) Expression of NMDA receptors in the thalamus. (D) Comparison of log–log scatter plot of expression of genes of pcd mice in the degenerating period (P60) for those in the pre-degenerating period (P40). The NMDA receptors subunits in the AC (blue diamonds), in the VC (red circles) and thalamus (green circles) were plotted. The AMPA receptors subunits in the AC (blue triangles) were also displayed. The ordinate and abscissa indicate the relative expression level of the receptor subunits that were compared to the expression of GAPDH. Pink lines indicate a 2-fold difference in expression. (E) Effect of systemic administration of MK801, an NMDA receptor antagonist, on spontaneous FO in the AC. The power spectrums before, 10 and 20 min after injection of MK801 were demonstrated. Scale bar = 0.1 mV^2/Hz in (E).

Appearance of fast oscillation (FO) in pcd mice

We further analyzed the frequency spectrum of spontaneous transcortical potentials (surface potential minus depth potential) in the ACs and VCs by fast Fourier transformation. Before P45, there were no clear differences between wt and pcd mice. After P45, we observed prominent FO at around 25 Hz in the AC of pcd mice (Fig. 3A, left and Fig. 3B, right column). The FO was not observed in the VC, wherein there is little degeneration in the thalamic relay neurons (Fig. 3A, right). We also did not find FO in wt mice after P45 (Fig. 3B, left column).

Expression of NMDA receptors in the AC and VC

As an initial step in determining the role of NMDA in the degeneration of thalamic neurons, we examined the expression of the NMDA receptors in the AC and VC before (P40) and during (P60) thalamic degeneration by the quantitative real-time PCR. We chose P40 as the pre-degeneration period because the developmental changes of NMDA receptors in the cortex terminate and become stable at this time [15] and because we did not observe morphological or electrophysiological changes at P40. The level of mRNA encoding the NMDA receptor subunits was

normalized by the level of GAPDH mRNA. The levels of NR1, NR2A, and NR2B mRNAs in the AC of pcd mice are significantly higher during the thalamic degeneration period (P60) compared to the period prior to thalamic degeneration (P40) (Fig. 4A; $P < 0.05$, Student's t-test). In contrast, there were no apparent changes in the expression of the NMDA receptor subunits in the VC during thalamic degeneration (Fig. 4B).

In the thalamus, we observed a general reduction in the level of mRNAs encoding the NMDA receptor subunits (Fig. 4C). The NR2D mRNA was not detected in the thalamus. This shows that the levels of NR2A and NR2B mRNAs were significantly down-regulated during degeneration ($P < 0.05$). Although not statistically significant, there was a trend for a decrease in the level of NR1 and NR2C mRNAs during degeneration. Finally, we did not observe significant changes for α-amino-3-hydoxy-5-methyl-4-isoxazole propionic acid (AMPA)-type glutamate receptor subunits (GluR1-3) in the AC or VC (Fig. 4D).

We found that systemic administration of MK801, an NMDA receptor antagonist, abolished FO in pcd mice (Fig. 4E). Local injection of MK801 into the thalamus, however, did not influence FO, whereas local injection of kynurenic acid, which blocks both AMPA and NMDA receptors, abolished it.

Discussion

In the current studies, we demonstrated that thalamic neurons including those in the MGv, the main relay station to the AC, degenerate in pcd mice. This finding agrees with previous reports using silver staining method [3,4]. We also confirmed that neurons in the dorsal medial geniculate and posterior intralaminar nuclei, which form the secondary auditory pathway, and those in the LGd, which organizes the main visual pathway, remain mostly intact. Analysis of DNA fragmentation and caspase 3 activation indicated that these neurons were undergoing apoptosis. We found that AEPs in pcd mice begin to decrease around P50 and amplitude of the AEPs reduce to about 40% by P60. This approximately agrees with a previous study demonstrating that degeneration begins around P50 and about 70% of the neurons in the MGv degenerate by P60 [4].

We observed an increase in the mRNA levels for NMDA receptor subunits in the AC but not in the VC or thalamus of pcd mice. This suggests that the FO is due to the enhanced activity of NMDA receptors in the AC. This was confirmed by the findings that systemic administration of MK801, an NMDA antagonist, abolished the FO. Involvement of NMDA receptors in generation of cortical oscillation has been reported by several other investigators. For example, Sebban reported that MK801 causes a marked reduction of the spectral power in higher frequencies of electroencephalograms recorded in the prefrontal cortex of the rat [16]. Also, NMDA receptor-dependent oscillation has been reported in the rat retrosplenial cortex [17].

Previous studies have shown that FO can be induced polysynaptically by thalamic stimulation in slices of the AC [18]. Note that neurons in the posterior intralaminar nucleus (PIL), an associative auditory thalamic nucleus, were spared from degeneration in pcd mice, whereas most of those in the MGv, the main auditory relay nucleus, degenerated. Interestingly, stimulation of the PIL but not the MGv has been shown to induce FO [19].

The accumulating evidence suggested that FO plays critical role of the genesis of symptoms of the neurodegenerative disease. In Parkinson's disease, FO is observed in the basal ganglia and cerebral cortex, and it was reported to be related to akinesia and tremor [20,21]. Akinesia and tremor can be reduced by the deep brain stimulation that is thought to desynchronize FO [22,23]. The current investigation clarified that the NMDA receptors are related to the generation of FO and the NMDA blocker extinguished it. These findings can serve to develop the new therapeutic strategies for the neurodegenerative diseases including Parkinson's disease.

Acknowledgments

This work was supported by the grants C1 and D of Kansai Medical University.

References

[1] R.J. Mullen, E.M. Eicher, R. Sidmann, Purkinje cell degeneration, a new neurological mutation in the mouse, Proc. Natl. Acad. Sci. USA 73 (1976) 208–212.
[2] S. Kyuhou, N. Kato, H. Gemba, Emergence of endoplasmic reticulum stress and activated microglia in Purkinje cell degeneration mice, Neurosci. Lett. 396 (2006) 91–96.
[3] S. O'Gorman, R. Sidman, Degeneration of thalamic neurons in "Purkinje cell degeneration" mutant mice. I. Distribution of neuron loss, J. Comp. Neurol. 234 (1985) 277–297.
[4] S. O'Gorman, Degeneration of thalamic neurons in "Purkinje cell degeneration" mutant mice. II. Cytology of neuron loss, J. Comp. Neurol. 234 (1985) 298–316.
[5] M. Steriade, E.G. Jones, R. Llinas, Thalamic Oscillation and Signaling, Wiley, New York, 1990.
[6] P. Bliss, G.L. Collingridge, A synaptic model of memory: long-term potentiation in the hippocampus, Nature 361 (1993) 31–39.
[7] N. Kato, H. Yoshimura, Reduced Mg2+ block of *N*-methyl-D-aspartate receptor-mediated synaptic potentials in developing visual cortex, Proc. Natl. Acad. Sci. USA 90 (1993) 7114–7118.
[8] H. Flohr, U. Lunenburg, Role of NMDA receptors in lesion-induced plasticity, Arch. Ital. Biol. 131 (1993) 173–190.
[9] L.C. Schmued, K.J. Hopkins, Fluoro-Jade B: a high affinity fluorescent marker for the localization of neuronal degeneration, Brain Res. 874 (2000) 123–130.
[10] K.B. Franklin, G. Paxinos, The Mouse Brain in Stereotaxic Coordinates, Academic Press, San Diego, CA, 1997.
[11] H.P. Cruikshank, P. Killackey, R. Metherate, Parvalbumin and calbindin are differentially distributed within primary and secondary subregions of the mouse auditory forebrain, Neuroscience 105 (2001) 553–569.
[12] G. Paxinos, L. Kus, K. Ashwell, C. Watson, Chemoarhchitectonic Atlas of the Rat Brain, Academic Press, San Diego, CA, 1999.
[13] L. Toso, S. Poggi, D. Abebe, R. Roberson, V. Dunlap, J. Park, C. Spong, *N*-Methyl-D-aspartate subunit expression during mouse

development altered by in utero alcohol exposure, Am. J. Obstet. Gynecol. 193 (2005) 1534–1539.
[14] S. Tajiri, S. Oyadomari, S. Yano, M. Morioka, T. Gotoh, J.I. Hamada, Y. Ushio, M. Mori, Ischemia-induced neuronal cell death is mediated by the endoplasmic reticulum stress pathway involving CHOP, Cell Death Differ. 11 (2004) 403–415.
[15] C. Hsieh, Y. Chen, F. Leslie, M. Metherate, Postnatal development of NR2A and NR2B mRNA expression in rat AC and thalamus, J. Assoc. Res. Otolaryngol. 3 (2002) 479–487.
[16] C. Sebban, B. Tesolin-Decros, J. Ciprian-Ollivier, L. Perre, M. Spedding, Effects of phencyclidine (PCP) and MK 801 on the EEG in the prefrontal cortex of conscious rats; antagonism by clozapine, and antagonists of AMPA-, alpha(1)- and 5-HT(2A)-receptors, Br. J. Pharmacol. 135 (2002) 65–78.
[17] H. Yoshimura, T. Sugai, M. Honjo, N. Segami, N. Onoda, NMDA receptor-dependent oscillatory signal outputs from the retrosplenial cortex triggered by a non-NMDA receptor-dependent signal input from the visual cortex, Brain Res. 1045 (2005) 12–21.
[18] R. Metherate, S.J. Cruikshank, Thalamocortical inputs trigger a propagating envelope of gamma-band activity in AC in vitro, Exp. Brain Res. 126 (1999) 160–174.
[19] D. Barth, K. MacDonald, Thalamic modulation of high-frequency oscillating potentials in auditory cortex, Nature 383 (1996) 78–81.
[20] A. Kühn, A. Kupsch, G. Schneider, P. Brown, Reduction in subthalamic 8–35 Hz oscillatory activity correlates with clinical improvement in Parkinson's disease, Eur. J. Neurosci. 23 (2006) 1956–1960.
[21] L. Timmermann, J. Gross, J. Dirks, L. Volkmann, H. Hans, A. Schnizler, The cerebral oscillatory network of parkinsonian resting tremor, Brain 126 (2003) 199–212.
[22] N. Fogelson, A. Kuhn, P. Silberstein, P.D. Limousin, M. Hariz, T. Trottenberg, A. Kupsch, P. Brown, Frequency dependent effects of subthalamic nucleus stimulation in Parkinson's disease, Neurosci. Lett. 382 (2005) 5–9.
[23] P. Brown, D. Williams, Basal ganglia local field potential activity: character and functional significance in the human, Clin. Neurophysiol. 116 (2005) 2510–2519.